Visual Image Retrieval and Localization

Yannis Kalantidis, Giorgos Tolias, Evaggelos Spyrou, Phivos Mylonas, Yannis Avrithis and Stefanos Kollias
Image, Video and Multimedia Systems Laboratory
National Technical University of Athens
School of Electrical and Computer Engineering
Iroon Polytexneiou 9, 15780 Zografou, Greece
Email: {ykalant, gtolias, espyrou, fmylonas, iavr}@image.ntua.gr, stefanos@cs.ntua.gr

***Abstract*—This paper suggests a content-based image retrieval scheme, applicable to large web collections. A fast and robust system is proposed, based on the popular bag-of-words model. SURF features are extracted from images and a visual vocabulary is created, through which images are efficiently represented. Furthermore, geometric constraints on the image features are taken into account, facilitating accurate retrieval. The performance of the proposed methods is evaluated on two common datasets, while an advanced web-based image retrieval application is presented, that yields a geographic position estimation about the query image, exploiting geotagged datasets.**

***Keywords*: image retrieval, geotags, localization, SURF, RANSAC, bag-of-words.**

I. Introduction

The popularity of social networks and web-based personal image collections has resulted to a continuously growing volume of publicly available photos and videos. Users are uploading, describing, taggging and annotating their personal photos. Moreover, a recent trend is to also ”geotag” them, that is to mark the location they were taken onto a web-based map. Consequently, this growth of image collections has created the need for fast, robust and efficient algorithms, able to analyze large-scale diverse and heterogeneous visual content. This growing need for automatic metadata generation, concept detection, search and retrieval has boosted research efforts towards these directions. The work presented herein is an approach that aims not only to retrieve visually similar images, but also to determine the location they were taken by exploiting the available socially created metadata. The proposed technique makes use of a visual vocabulary and a bag-of words approach, in order to describe the visual properties of an image. Moreover, geometric constraints are applied, in order to extend the bag-of-words model towards more accurate results.

Numerous extensions to the bag-of-words approach have been proposed recently. For example, [1] explores techniques to map each visual region to a weighted set of words, allowing the inclusion of features which were lost in the quantization stage of previous systems. The set of visual words is obtained by selecting words based on proximity in descriptor space. In [2], images are segmented into regions, regions are classified into visual words, using a variety of features. Then a mapping between visual words and keywords is learned using an EM method. In [3], an approach for the linguistic indexing of images is presented, that uses Wavelets to extract image features and Hidden Markov Models (HMMs) to learn the association of those features to the keywords describing the images. [4] proposes a randomized data mining method that finds clusters of spatially overlapping images. This unsupervised method is applied on large databases and finds clusters of similar regions and also is capable to retrieve near-duplicates of images. Moreover, the approach of [5] uses a visual words' description of images and then tries to create a more accurate description by using Hamming embedding and weak geometric consistency constraints.

While global extraction of features and local from regions presents good results in certain retrieval problems, in the case of ”object”-based applications they present serious limitations. Thus, most modern algorithms begin with the determination of some interest points within an image. These points carry some properties such as invariance to various image transformations, illumination etc. They continue by defining regions in the neighborhood of these points and extract the descriptors within them. We should note here, that while some of the papers presented herein deal solely with object detection, the techniques mentioned are also important in the area of image retrieval, when the goal is to retrieve images based on the objects/places they contain. In [6], a representation of local image structure and a matching scheme, both insensitive to many appearance changes is presented. This method is applied on two-view matching problems of images from different modalities. Moreover, [7] presents a method to learn and recognize object class models from unlabeled and unsegmented cluttered scenes in a scale invariant manner. In this work, objects are modeled as flexible constellations of parts. A probabilistic representation is used for all aspects of the object: shape, appearance, occlusion and relative scale. An entropy-based feature detector is then applied for region selection within the image. Also, in [8], object recognition is based on affine invariant regions. Segmentation and

Y. Kalantidis is an undergraduate student, working on image indexing and retrieval. G. Tolias is a PhD Candidate working on image retrieval and object recognition. E. Spyrou is a PhD Candidate working on semantic multimedia analysis. Ph. Mylonas is a researcher in the fields of personalization and context modelling. Y. Avrithis is a senior researcher in the field of multimedia analysis. Professor S. Kollias' research interests include image and video processing, analysis, coding, storage, retrieval, multimedia systems, computer graphics and virtual reality, artificial intelligence, neural networks, human computer interaction and medical imaging.

recognition are achieved simultaneously. In [9], the problem of near-duplicate image retrieval is tackled with a parts-based representation of images using distinctive local descriptors extracted from points of interest, which are invariant under several transformations. Moreover, the work presented in [10], uses parts affinely rigid by construction. Object detectors are trained by identifying groups of neighboring local affine regions whose appearance and spatial configuration remains stable across multiple instances. In [11], a novel feature matching method aims to tackle efficiently high-dimensional problems. The work presented in [12] is a large-scale object retrieval system. Therein, the query is a region of an image and the system retrieves images that contain the same object as the one contained in the user's query.

The architecture of the presented system is depicted in Fig. 1. In the *offline* procedure (Fig. 1(a)), a visual vocabulary is created, in such a way that contains the most common visual local patterns of the dataset. Each database image is afterwards represented in terms of this visual vocabulary through a model vector. This process takes place only once and for all the images of the given database. In the *online* procedure(Fig. 1(b)), the user uploads or chooses a query image from the database. From this image, points of interest and visual descriptors are extracted and the model vector representing the image is calculated using the same process. By comparing the model vector to those of the database, the system retrieves similar images.

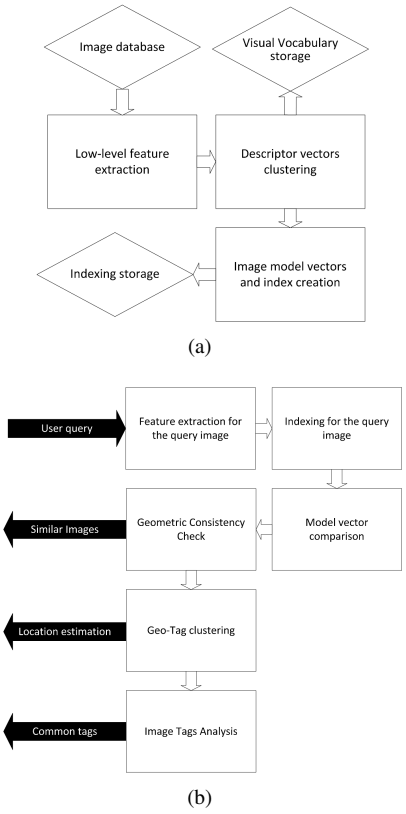

Fig. 1. The architecture of the proposed retrieval system. Online (1(a)) and offline (1(b)) process.

This paper is organised as follows: Section II presents the local features extracted from images. The process of creating a visual vocabulary and indexing is presented in Section III. The matching procedure between two images is described in Section IV followed by the geometric consistency check in Section V. The implemented application that locates an image is presented in Section VI followed by further experimental retrieval results in Section VII. Finally, conclusions and plans for future work are drawn in Section VIII.

II. Local features

For the representation of the visual content of a given image a set of interest points is selected and visual features are extracted locally, from their surrounding area. Since the goal is to choose scale invariant interest points, their localization is carried out on a gaussian scale-space. In this work, the SURF (Speeded-Up Robust Features)[13] features have been selected to capture the visual properties of the images. These features have been proven to achieve high repeatability and distinctiveness. Apart from that, their extraction speed is very fast, when compared e.g. with the SIFT features [14]. An example of the extracted SURF features is depicted in figure 2.

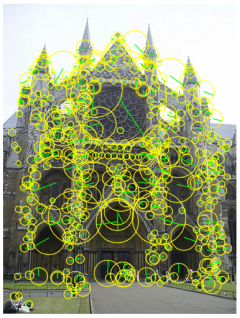

Fig. 2. Interest points extracted with the SURF Fast Hessian detector. The size of the yellow circle and the green line denote the scale and the dominant orientation, respectively.

For the localization of interest points, a fast approximation of the Hessian matrix is adopted, which exploits the use of integral images. Then the local maxima of the Hessian matrix determinant are chosen as interest points. This blob response maxima process is carried out on several octaves of a Gaussian scale-space. The correct scale is automatically selected also from the Hessian determinant, as introduced in [15]. For the exact point localization, an efficient non-maximum suppression algorithm is used at a $3 \times 3 \times 3$ intra-scale neighbourhood [16].

The SURF descriptor captures the intensity content distribution around the interest point detected with the aforementioned process. The first order Haar wavelet responses are computed with the use of integral images, resulting to a 64-dimensional feature vector. In order to achieve rotation invariance, a dominant orientation is determined. This is selected as the direction that maximizes

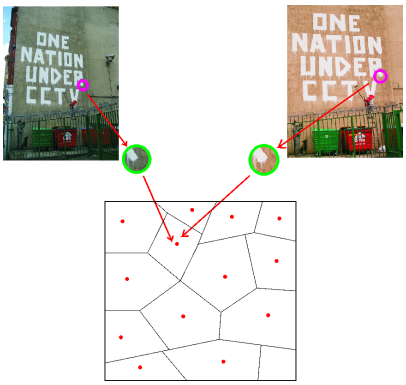

Fig. 3. Two points extracted from different images, corresponding to the same visual word.

the sum of the Haar-wavelet responses in a sliding window of size $\pi/3$ around the interest point neighborhood.

To compute the descriptor, a square area around the interest point with $20 \times s$ side length is selected is divided in 4×4 blocks, with s denoting the interest point scale. Thus, the descriptor is also scale invariant. At each one of the 16 blocks, 4 values that correspond to the sum of the x,y, $|x|$ and $|y|$ first order Haar wavelet responses in a 5×5 grid in the block are extracted. To make the descriptor robust to contrast changes, the descriptor vector is turned into a unit vector.

III. Visual Vocabulary and Indexing

To understand the notion of a visual vocabulary, one should consider it as an equivalent to a typical language vocabulary, with an image corresponding to a part of a text. In the same way that text may be decomposed to a set of words, an image can also be decomposed to a set of *visual* words. Then, in order to compare two images, their corresponding visual words may be compared. Thus, it is interesting to create a visual vocabulary in such a way that parts of images could be meaningfully assigned to visual words. Fig. 3 depicts two regions of interest extracted from two different images, that correspond to the same visual word. The visual vocabulary is presented as the Voronoi cells of the clustered space of visual words. We should note here that due to their polysemy, visual words cannot be as accurate as natural language words.

A. Visual Vocabulary Construction

To create the visual vocabulary, a clustering process is followed. More specifically, the well-known K-means clustering algorithm [17] is applied on the SURF descriptors corresponding to a very large number of points of interest. If the number of the points to be clustered is significantly large, clustering using the K-means algorithm becomes a very slow task. For example, clustering of 5M of points (which are typically extracted from 10K of images) requires a few days of processing. However, to efficiently deal with large scale retrieval problems, the size of the vocabulary should be in the order of a few tenths of thousands of visual words [18],[19]. Thus, in order to rapidly create an appropriate vocabulary, the clustering process is performed on a smaller subset, carefully selected to contain the most representative images. After constructing the visual vocabulary, each image has to be represented with a description that captures its relation to all the words of it. We should also emphasize here that in order to create a visual vocabulary able to perform well in more than one domains, the images from which the regions of interest are extracted, have to be an diverse and as possible heterogeneous and moreover its size has to be significantly large.

B. Nearest Neighbor search using a k-d tree

For the model vector formulation, we need to find the visual word that is the closest in terms of descriptor vector to each one of the image's points. To do this fast and efficiently we rely on the k-d tree structure. The structure of k-d trees has been widely used in information retrieval during the last decades [20], [21]. This data structure is a binary tree, which stores a finite number of k-dimensional data points and has been widely applied in the field of computer learning [22] and neural networks [23]. Within the presented work, k-d trees are used in order to find the closest visual word of every point of interest, which is typically a very difficult and time consuming task due to the large dimension of points.

Given N k-dimensional elements, the k-d tree is constructed by partitioning the space iteratively, one dimension at a time. At each iteration, the feature space is divided into two subspaces along the selected dimension. This process is repeated until each subspace contains a single point. This process creates a tree which allows a very fast search for all data points. The height of this tree is $log(n)$.

In the case of the presented work, a k-d tree is created by the centroids of the clusters that are created by the clustering process. The dimension of the centroids is equal to 64. These centroids comprise the visual words of the visual vocabulary. This tree is created once and for all the images that we would like to index. Then, within the process of formulating the model vector, for each point of the given image, its nearest neighbor is determined using the k-d tree.

C. Model Vector Formulation

After constructing the visual vocabulary, a given image is represented in terms of it using a (*Model Vector*). To each descriptor of an image point, the most similar visual word of the vocabulary is assigned. Then, a histogram is constructed for each image, which counts the occurrences of the visual words of the vocabulary within it. A visual word is said to occur to an image if it is the nearest neighbor of all points within the image. We can write for the model vector of the image I as a N_{vw}-dimensional vector, where N_{vw} is the size of the visual vocabulary, like

$$mv_I = \left[tf_I(0), tf_I(1), \ldots, tf_I(N_{vw})\right] \quad (1)$$

where $tf_{I,i}$ denotes the number of times that the visual word i was selected as a nearest neighbor of one of the image I interest points. In order to find the closest visual word to a

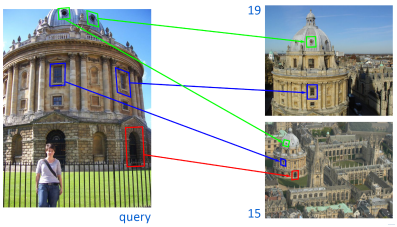

(a)

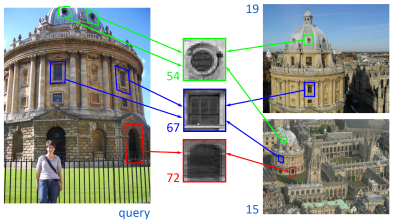

(b)

Fig. 4. Matching of two images without a visual vocabulary (4(a)) and with a visual vocabulary (4(b)).

point, the aforemention k-d tree structure is used, with the tree created for the visual vocabulary centroids-words.

The histogram of visual word appearance frequencies is then normalized and its non-zero values are stored in an index which resembles to the technique of inverted files, widely used to fast text retrieval [24],[25]. Each image is then represented by its corresponding visual words and the frequencies they occur. From this point, when it is mentioned that a visual word appears within an image, this would mean that this visual word is the nearest neighbor of one or more of the image's interest points.

In presence of large vocabularies of over 10^4 visual words, the model vector is very sparse. It can have at most as many non zero values as the image's interest points, when every one of them is assigned to a different visual word. So, in practice, only the non-zero values of the model vector are stored to save storage and gain speed.

Since this indexing process is inspired by techniques applied in the task of text search, in addition to the term frequency (tf), which is the frequency of a given term in a document, inverse document frequency (idf), can also be used. This case is studied in section III-D.

The process of querying an image database without and with a visual vocabulary is depicted in Fig. 4. In the first case the comparison of the local descriptors is performed immediately for two images and after exhaustive comparisons in the whole database, the closest regions are found. In the latter case, for every image of the database all points have been assigned to appropriate visual words of the visual vocabulary. Thus, for a new query, its points have to be assigned to the closest visual words of the vocabulary. After this process, two images are considered to be similar if their points are assigned to similar visual words.

D. Inverse Document Frequency and Stop List

Inverse Document Frequency is another technique used in information and text retrieval [26], which during the last few years has been applied to image retrieval, either along with language processing [27], or using visual dictionaries [28] [29].

The model vector of an image has taken, up to now, only the frequency of the appearance of a visual word as a nearest neighbor to any of the interest points into account. We define the *Inverse Document Frequency* or *idf* as:

$$idf_k = log\frac{N}{n_k} \tag{2}$$

where N is the total number of the images of the given collection (the size of the database) and n_k the number of the appearences of the visual word VW_k as the nearest neighbor to all points of all images in the database. Thus, idf acts as a weighting scheme, which identifies the most and less frequent visual words of the entire collection. The model vector can now be formulated as:

$$mv_I = \left[(tf_I(0)*idf_0), (tf_I(1)*idf_1), \ldots, (tf_I(N_{vw})*idf_{N_{vw}})\right] \tag{3}$$

with idf_k being the idf value of the visual word k.

It is obvious that the most common visual words, the ones with the smallest idf values, are not discriminative and their absence would facilitate retrieval. On the other hand, the rarest visual words are in most of the cases a result of noise and can be distracting to the retrieval. To overcome these problems, in some cases a stop list is created that includes the most and the least frequent visual words of the image collection. Using this list, the presence of its visual words is ignored, thus resulting to even sparser model vectors and smaller image representations.

IV. Matching

In order to compute the similarity between images, two similarity measures are used. The first one is the most commonly used inner product of the model vectors. If mv_q and mv_{db} are the model vectors for the query image I_q and a database image I_{db} respectively, their matching score can be computed with

$$sim_{prod}(I_q, I_{db}) = \sum_{i=0}^{N_{VW}} mv_q(i)mv_{db}(i) \tag{4}$$

where N_{VW} is the visual vocabulary size, and $mv_x(i)$ corresponds to the value or term frequency of the visual word i in image x. The second similarity measure is histogram intersection, discussed also in [29]. Regarded as histograms, the similarity of the two model vectors for the query and a database image can be computed as:

$$sim_{hist}(I_q, I_{db}) = \sum_{i=0}^{N_{VW}} \min(mv_q(i), mv_{db}(i)) \tag{5}$$

For both matching measures, and since the vectors can be very sparse, the inverted file scheme is used in order to decrease matching time.

When a user query reaches the system, then the local low-level features are extracted from the query image and the model vector is computed. Then the similarity of the query model vector with all database model vectors is computed, and the N most similar images, the images with the highest such value, are either returned to the user as similar, or become candidates for geometric consistency check, as explained below.

V. Geometric Consistency Check

When the retrieval process considers only the model vectors that represent the visual content of images, sometimes fails to produce accurate results. This is because the bag-of-features approach totally ignores the geometry of the extracted interest points. Two images can contain similar visual words, but in a totally different spatial layout one from the other. Thus, the inclusion of a geometry consistence check would be very useful. The method that was adopted is the RANSAC algorithm [30]. This method can find the homography between two images given a set of tentative point-to-point correspondences, in presence of many false such correspondences that are also called *outliers*. In fact the RANSAC algorithm estimates the homography that maximizes the number of *inliers* that is the set of correspondences that support the model.The ransac algorithm is described in section V-A.

It is obvious that RANSAC algorithm as presented before, relies a lot in the correspondences of the points, which will be provided initially. These correspondences are not available, thus need to be calculated. A method that finds the nearest neighbors is not efficient, since it is a very time-consuming procedure that needs to be computed online. However, we can exploit the correspondences between points and visual words, in order to create tentative point correspondences between two images. This requires an additional indexing process, according to which, for every image and every visual word that appears in it, we store the locations of the points that yield this visual words as nearest neighbor. We should note here that this process is very fast.

This procedure, however, introduces many false correspondences, due to the quantization effect of the bag-of-words approach. So if for example a visual word appears 4 times in one image and 5 in the other, then with out method $4 \times 5 = 20$ correspondences will be formed, instead of 4 correct ones. Taking this into account, a rejection procedure follows, called *neighbor check*, that rejects correspondences between points whose neighborhoods does not match[28]. This means that in order to keep a tentative correspondence as valid, we require some of its spatially neighboring points to also have a valid correspondence between them. An example of the RANSAC inliers between two images in the presence of partial occlusion is shown in Fig. 5.

Since this method is computationally expensive, we choose not to apply it in the whole database, but in the most similar images, in terms of their model vectors. It is important to clarify that RANSAC does not retrieve images but *re-ranks* them, based on the spatial layout of their interest points. This approach appears to minimize the number of false positives. Using an appropriate threshold on the retrieved results, a higher precision can be easily achieved.

Fig. 5. The RANSAC inliers found between the two images.

A. Homography estimation using RANSAC

The well known RANSAC (RANdom SAmple Consensus) algorithm is applied between two images in order to determinate the homography between them, in presence of many outliers. By homography, we mean the perspective transform that maps any given point x_i of the first to the corresponding point x_i' of the latter. Given the set of correspondences between two images, that is the pairs $x_i \leftrightarrow x_i'$, we can define the homography matrix H as:

$$x_i' = H x_i \tag{6}$$

In general, estimating this homography has proven very useful in tasks such as stereoscopic camera calibration, a case where the images captured by both cameras differ only by means of a perspective transform. This simple idea is extended herein and instead of the two images taken by a stereoscopic camera, we consider the case of the same object captured by different points of views. We should expect that in this case the the homography will result to a large number of false correspondences since the variation of the viewpoint is significantly higher. To overcome this, the RANSAC algorithm is applied, since it is able to estimate correctly the homography even with a large number of false correspondences present. The goal of this method is not only to estimate the homography matrix, but also to classify the points into two categories: Those that represent correct correspondences (inliers) and those that represent false correspondences (outliers).

In general, when the goal is to fit a model into data, our initial random sample should contain a number of points equal to the number of the model variables. In the homography case, the model requires at least 4 initial points. Given the correspondences of the points between two images, the basic RANSAC algorithm that makes an estimation of the homography between two images is as follows:

- 4 points are selected in a random manner. This is the minimum number of points needed to define a homography. These points are initially assumed to be inliers.
- Using the model that was estimated during the previous step and a distance parameter t, the number of the points that satisfy the model is calculated. Their distance to the point estimated by the homography model should be smaller than the predefined threshold t:

$$d^2_{vertical} < t^2 \tag{7}$$

  where $t^2 = F_m^{-1}(\alpha)\sigma^2$ and $F_m(k^2) = \int_0^{k^2} \chi^2_m(\xi)d\xi$ denote the probability density distribution for the error, which we assume that follows χ^2_m with m degrees of freedom. The points for which the aforementioned relation stands are the inliers of the model. A typical value for α is 0.95. This means that the probability that a given point is an inlier is equal to 95%.
- random quadruplets of points are sampled repeatedly, and after every iteration the maximum number of inliers up to that point is kept together with the corresponding model.
- This process is repeated until a predefined number of iterations is reached, or the value of the probability that new inliers could be found using another model falls beneath $\eta\%$. This probability is defined as:

$$\eta = (1 - P_I)^k \tag{8}$$

  where k denotes the number of the correspondences between two images and P_I is the probability that a sample consisting solely from inliers is selected:

$$P_I = \frac{\binom{I}{m}}{\binom{N}{m}} = \prod_{j=0}^{m-1} \frac{I-j}{N-j} \approx \epsilon^m \tag{9}$$

  $\epsilon = I/N$ denotes the ratio inliers / points. A typical value for ϵ is equal to 0.99.
- When the aforementioned relation is satisfied, the homography model is redefined, using all inliers selected from the previous steps.

VI. Application: Geographical Location of Images

During the last few years one of the trends in the image collections of the World Wide Web is the inclusion of metadata which aim to provide a more complete description. Typical metadata contain a free text description, some representative tags and some metadata related to the geographical position that the image was taken (Geo-tag). A *Geo-tag* consists of the geographic coordinates: the longitude and the latitude, and is either extracted automatically through GPS from some cameras or manually defined by the user. In the latter case case, users mark their position on a map, using web-based applications. A very popular example is Flickr[1]. It is estimated that each month, almost 3M of geotagged images are uploaded.

If a user queries with a landmark image in a large database of Geo-tagged images, then the top retrieved results will probably contain the landmark that the query image depicts. Those correctly retieved images are expected to have near identical Geo-tag values. Little variance is expected since geo-data can be defined by users and also because the same building can be photographed by different distances (using the appropriate camera lens). However, the estimated Geo-tag for the query image is expected to be within the larger consistent subset of the result images.

Several experiments have been performed in a collection of 2000 images collected from Flickr, depicting monuments and characteristic buildings of London. These images have been selected as the most representative of those buildings, within a set of 20000 downloaded images. We should note that all images used in the experiments had been geotagged by Flickr users.

Within the implemented application, a user is able to execute a query of an image depicting among others a monument of London. The system responds not only with visually similar images, but also with an estimation of the location of the query image, and frequent tags that can accompany it.

To find the most consistent subset mentioned above, an agglomerative clustering algorithm is used, on the 2-dimensional geographic coordinates of the retrieved images. An agglomerative clustering merges in one the points that lay in distance closer to a predefined value t. Setting t to represent the area around a building or monument, each cluster of Geo-tags will denote a location. The query landmark images, that are in most of the times a large subset of the retrieved results, will probably yield the largest cluster. The algorithm used herein is the Reciprocal Nearest Neighbor (RNN) [31],[32].

Images uploaded by users contain free text annotation in terms of tags describing the visual content of the image. This information can be exploited to provide the the user with some tag recommendations for an image query. Using a stop list analogy the most and less frequent tags are suppressed and the most common tags in the final set of retrieved images are the system's tag recommendations.

To visualize the query results, the graphical interface of the Google Maps application has been used, as depicted in Fig. 6. In this map, the red marker denotes the geographical position of the query image, and the blue markers denote the positions of the images that match the query in terms of their visual features. Some indicative retrieval results are also presented in Fig. 7. Apart from the visual features of the retrieved images, their most common tags have been also extracted. Those tags are depicted in Fig 6.

VII. Experiments

To evaluate our method, we perform experiments on two publicly available annotated datasets. The *Zurich Buildings* dataset[2], and the *Recognition benchmark images* dataset[3] [33]. The Zurich Buildings dataset contains 1005 images picturing buildings of the city of Zurich. Each buildings is portrayed

[1] http://www.flickr.com

[2] http://www.vision.ee.ethz.ch/datasets/index.en.html

[3] http://www.vis.uky.edu/~stewe/ukbench/

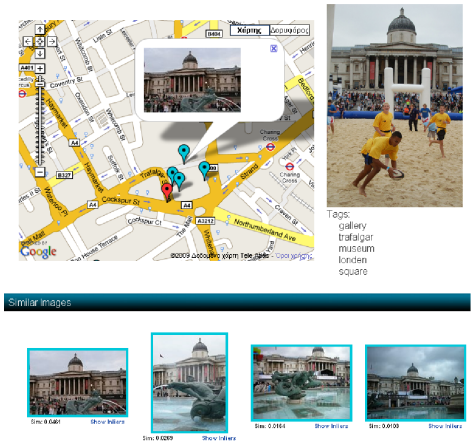

Fig. 6. Upper row: A Google map is depicted on the left, estimating the location of the query image depicted on the right. Under these images, the most common tags are estimated. Lower row: Visually similar retrieved images.

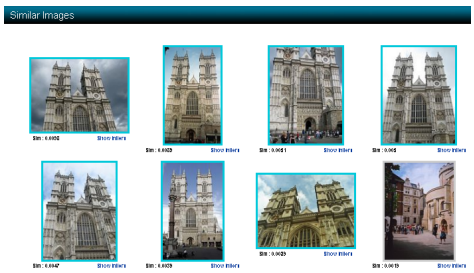

Fig. 7. Query Results. Images that are estimated to be in the same location of the query image have a light blue border.

in 5 images, resulting to a total of 201 buildings. The Recognition benchmark images dataset consists of 10200 images of everyday objects, with 4 images for each one. A representative sample of the two dataset images is depicted in Fig.8 and Fig.9 respectively.

As mentioned before, the local features extracted are the 64-dimensional *SURF* detector and descriptor [13], features that guarantee scale and rotation invariance. For the geometric consistency check, RANSAC is used, on a fractal of the top-ranked results of the baseline method.

The method was tested by performing queries with every image in the dataset. We measure the average precision for each query and get the mean on the average precisions of each one of the object/building queries. Furthermore, the recall rate r_R was evaluated, which is defined as $r_R = \frac{n_R}{R}$, where n_R is the number of correct answers in the first R retrieved images. R equals to 5 for the Zurich Buildings and to 4 for the Recognition benchmark images dataset.

Experiments were carried out using different vocabulary sizes and both with product matching and histogram intersection. A summarization of the results is shown in figures 10(a) and 10(b) for the two datasets respectively, showing the mean average precision metric achieved for vocabularies varying from 1000 to 40000 visual words.

Fig. 8. Images from the Zurich Buildings dataset.

Fig. 9. Images from the UKBench Buildings dataset.

To simulate large-scale image search, many *distractor* images were added to the Zurich Buildings dataset. These images are images from other datasets containing diverse content, from buildings to objects. This way, the ratio of correct results to the total number of images decreases even more, and has a value less than 10^{-4}. The measured results showed, that this addition of many distractor images didn't affect the final performance much, and it still maintains high levels.

In table I the average recall rate as described above is shown for the three datasets.

Dataset	Average Recall
Recognition Benchmark Images	0.73
Zurich Buildings	0.8506
Zurich Buildings + Distractor Images	0.766

TABLE I
THE AVERAGE RECALL RATE, FOR THE FIRST 5 AND 4 RESPECTIVELY, TOP RETRIEVED IMAGES.

VIII. Conclusions and Future Work

In this paper we presented an approach on image retrieval and localization. We showed how the bag-of-words model can be extended by adding geometrical consistency, and how geotags can be exploited in order to allow localization. Future work will include application to larger sets of images, improvements of the geometrical consistency model in terms of speed and accuracy and extensions of the presented algorithm in order to be used in the task of object recognition.

Acknowledgments

This research was partially supported by the European Commission under contract FP7-215453 - WeKnowIt.

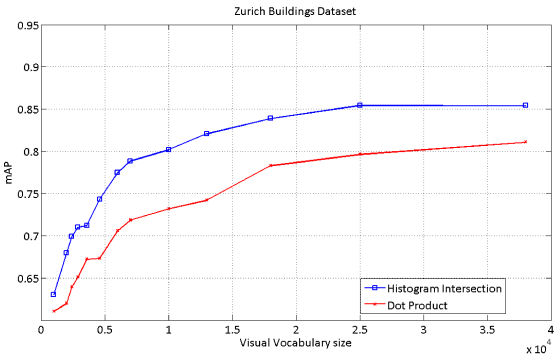

(a)

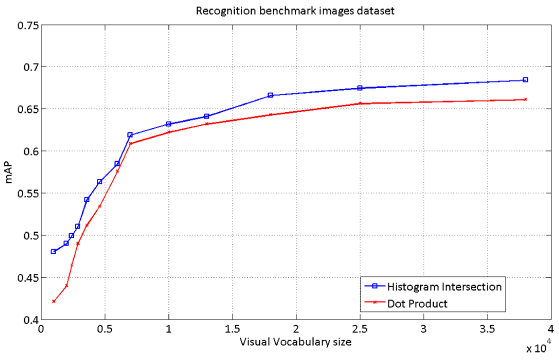

(b)

Fig. 10. The mean Average Precision metric for the two datasets, using product (red line) and intersection (blue line) as the matching method.

Evaggelos Spyrou is partially funded by PENED 2003 Project Ontomedia 03ED475.

REFERENCES

[1] J. Philbin, O. Chum, M. Isard, J. Sivic, and A. Zisserman, "Lost in quantization improving particular object retrieval in large scale image databases," *Image*, vol. 9, no. 14, pp. 15–17.

[2] P. Duygulu, K. Barnard, J. De Freitas, and D. Forsyth, "Object recognition as machine translation: Learning a lexicon for a fixed image vocabulary," *Lecture Notes in Computer science*, pp. 97–112, 2002.

[3] J. Li and J. Wang, "Automatic linguistic indexing of pictures by a statistical modeling approach," *IEEE TRANSACTIONS ON PATTERN ANALYSIS AND MACHINE INTELLIGENCE*, vol. 2, pp. 1075–1088, 2003.

[4] O. Chum and J. Matas, "Web scale image clustering: Large scale discovery of spatially related images," Technical Report CTU-CMP-2008-15, Czech Technical University in Prague, 2008, Tech. Rep.

[5] H. Jegou, M. Douze, and C. Schmid, "Hamming embedding and weak geometric consistency for large scale image search," *ECCV, Oct*, 2008.

[6] O. Chum and J. Matas, "Geometric hashing with local affine frames," in *Computer Vision and Pattern Recognition*, vol. 1, 2006, pp. 879–884.

[7] R. Fergus, P. Perona, and A. Zisserman, "Object class recognition by unsupervised scale-invariant learning," in *Computer Vision and Pattern recognition*, vol. 2. IEEE Computer Society; 1999, 2003, pp. 1575–1589.

[8] V. Ferrari, T. Tuytelaars, and L. Van Gool, "Simultaneous object recognition and segmentation from single or multiple model views," *International Journal of Computer Vision*, vol. 67, no. 2, pp. 159–188, 2006.

[9] Y. Ke, R. Sukthankar, and L. Huston, "Efficient near-duplicate detection and sub-image retrieval," in *ACMA C Multimedia*, vol. 9, no. 14. IEEE Computer Society; 1999, 2004, pp. 869–876.

[10] S. Lazebnik, C. Schmid, and J. Ponce, "Semi-local affine parts for object recognition," in *British Machine Vision Conference*, vol. 2, 2004, pp. 959–968.

[11] D. Omercevic, O. Drbohlav, and A. Leonardis, "High-dimensional feature matching: Employing the concept of meaningful nearest neighbors," in *Ieee 11Th International Conference on Computer Vision*, 2007, pp. 1–8.

[12] J. Philbin, O. Chum, M. Isard, J. Sivic, and A. Zisserman, "Object retrieval with large vocabularies and fast spatial matching," in *Proc. C V P R*, vol. 3613, 2007, pp. 1575–1589.

[13] H. Bay, A. Ess, T. Tuytelaars, and L. V. Gool, "Speeded-up robust features (surf)," *Comput. Vis. Image Underst.*, vol. 110, no. 3, pp. 346–359, 2008.

[14] D. G. Lowe, "Distinctive image features from scale-invariant keypoints," *Int. J. Comput. Vision*, vol. 60, no. 2, pp. 91–110, 2004.

[15] T. Lindeberg, *Scale-Space Theory in Computer Vision*. Kluwer Academic Print on Demand, 1994.

[16] A. Neubeck and L. Van Gool, "Efficient Non-Maximum Suppression," in *Pattern Recognition, 2006. ICPR 2006. 18th International Conference on*, vol. 3, 2006.

[17] J. MacQueen, "B. 1967.Some methods for classification and analysis of multivariate observations," in *Proceedings of 5th Berkeley Symposium on Mathematical Statistics and Probability*, pp. 1–297.

[18] H. Jegou, M. Douze, and C. Schmid, "Hamming embedding and weak geometric consistency for large scale image search," in *European Conference on Computer Vision*, ser. LNCS, A. Z. David Forsyth, Philip Torr, Ed. Springer, oct 2008, to appear. [Online]. Available: http://lear.inrialpes.fr/pubs/2008/JDS08

[19] J. Philbin, O. Chum, M. Isard, J. Sivic, and A. Zisserman, "Object retrieval with large vocabularies and fast spatial matching," in *Proc. CVPR*, 2007.

[20] J. Freidman, J. Bentley, and R. Finkel, "An Algorithm for Finding Best Matches in Logarithmic Expected Time," *ACM Transactions on Mathematical Software (TOMS)*, vol. 3, no. 3, pp. 209–226, 1977.

[21] J. Bentley, "Multidimensional binary search trees used for associative searching," *Communications of the ACM*, vol. 18, no. 9, pp. 509–517, 1975.

[22] A. Moore, "An intoductory tutorial on kd-trees," Technical Report, Tech. Rep.

[23] S. Omohundro, "Efficient algorithms with neural network behavior," *Complex Systems*, vol. 1, no. 2, pp. 273–347, 1987.

[24] D. Squire, W. Müller, H. Müller, and T. Pun, "Content-based query of image databases: inspirations from text retrieval," *Pattern Recognition Letters*, vol. 21, no. 13-14, pp. 1193–1198, 2000.

[25] I. Witten, A. Moffat, and T. Bell, *Managing Gigabytes: Compressing and Indexing Documents and Images*. Morgan Kaufmann, 1999.

[26] Y. Rui, T. Huang, and S. Mehrotra, "Content-based image retrieval with relevance feedback in MARS," in *Image Processing, 1997. Proceedings., International Conference on*, vol. 2, 1997.

[27] M. Kanade, "Video Skimming and Characterization through the Combination of Image and Language Understanding," in *Proceedings of the 1998 International Workshop on Content-Based Access of Image and Video Databases (CAIVD'98)*. IEEE Computer Society Washington, DC, USA, 1998, p. 61.

[28] J. Sivic and A. Zisserman, "Video google: A text retrieval approach to object matching in videos," in *ICCV '03: Proceedings of the Ninth IEEE International Conference on Computer Vision*. Washington, DC, USA: IEEE Computer Society, 2003, p. 1470.

[29] O. Chum, J. Philbin, and A. Zisserman, "Near duplicate image detection: min-hash and tf-idf weighting," in *Proceedings of the British Machine Vision Conference*, 2008.

[30] M. Fischler and R. Bolles, "Random sample consensus - a paradigm for model fitting with applications to image analysis and automated cartography," *Communications of the ACM*, vol. 24, no. 6, pp. 381–395, 1981.

[31] C. Olson, "Parallel algorithms for hierarchical clustering," *Parallel Computing*, vol. 21, no. 8, pp. 1313–1325, 1995.

[32] B. Leibe, A. Leonardis, and B. Schiele, "Robust Object Detection with Interleaved Categorization and Segmentation," *International Journal of Computer Vision*, vol. 77, no. 1, pp. 259–289, 2008.

[33] D. Nister and H. Stewenius, "Scalable recognition with a vocabulary tree," in *Computer Vision Pattern Recognition*, 2006, pp. 2161–2168.